A REVIEW OF NUCLEAR MICROSCOPY AND APPLICATIONS IN MEDICINE

P S P Thong, J Makjanic, F Watt

ABSTRACT

Nuclear Microscopy, the extraction of analytical information from microscopic regions of a sample using a scanning focused high energy ion beam, has been increasing in popularity recently, despite its technical complexity. The three ion beam related techniques Particle Induced X-ray Emission (PIXE), Rutherford Backscattering Spectrometry (RBS) and Scanning Transmission Ion Microscopy (STIM) can be carried out simultaneously at sub-micron spatial resolutions, and provide structural and quantitative elemental analysis down to the parts per million levels of analytical sensitivity. These techniques are extremely useful for measuring any imbalances in trace elements, including metal ions, in localised regions of biological tissue, and as such can provide unique information on many diseases. In this paper we briefly describe the nuclear microscope and its related ion beam techniques, and briefly review recent work carried out using the nuclear microscope into the degenerative diseases Alzheimer's disease, Parkinson's disease and atherosclerosis.

Keywords: nuclear microscopy, Alzheimer's disease, Parkinson's disease, atherosclerosis
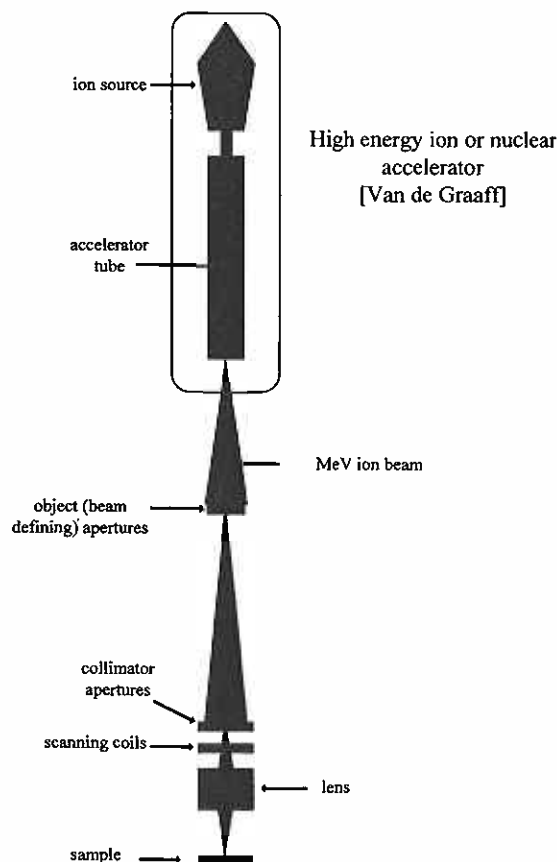
INTRODUCTION

The use of a focused beam of high energy ions to extract analytical information from biological tissue is a relatively recent development. The requirements of a multi-million volt nuclear accelerator to produce the high energy ions, together with a complex magnetic quadrupole multi-lens system to focus the ions into a small spot size, have limited the availability of this technique mostly to Physics Departments specialising in low energy nuclear physics. Nevertheless, in spite of the technological complexities of the nuclear microscope, the number of nuclear microscope groups around the world engaging in biomedical research is steadily increasing.

The nuclear microscope relies on the interaction between a scanning high energy ion beam probe (usually 2-4 MeV protons) and the specimen. A schematic diagram of the nuclear microscope is shown in Fig 1; a demagnified image of a high energy ion beam illuminating a small object aperture is used as a probe for extracting information from the specimen. In this paper, we shall deal with three ion beam related techniques which are relevant to biomedical research (Fig 2):

a) Particle Induced X-ray Emission (PIXE)[1]

When a high energy ion (eg a proton) collides with matter, there is a high probability that an inner core electron from an atom in the sample is knocked out of its orbit. The vacancy in the electron shell is immediately filled by an electron from an adjacent

Nuclear Microscopy Group
Department of Physics
National University of Singapore
10 Kent Ridge Crescent
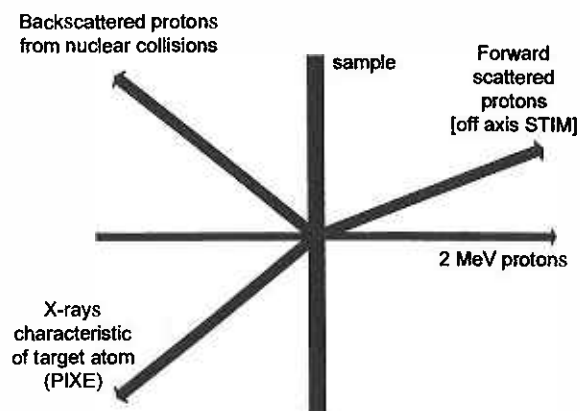**Singapore 119260**

P S P Thong, MSc
Research Assistant

J Makjanic, PhD
Research Assistant

F Watt, PhD
Associate Professor

Correspondence to: Ms P S P Thong

Fig 1 – Schematic diagram of a scanning nuclear microprobe (nuclear microscope).

electron shell, which is accompanied by a corresponding release of energy characteristic of the parent atom. For example, the characteristic energy released from a calcium atom is a single X-ray photon of energy 3.7 keV, and from an iron atom is an X-ray of energy 6.4 keV. Measurement of the energies of X-rays emanating from a sample under bombardment from high energy

Fig 2 – Main proton/sample interactions used in nuclear microscopy.

Fig 3 - X-ray energy spectrum of a pollen tube (CTC treated, fixed with glutaraldehyde and air dried) taken with (a) an electron microprobe operating at an energy of 10 keV, and (b) the Heidelberg proton microprobe at an excitation energy of 2.5 MeV. *(Reproduced with the kind permission of K Traxel.)*

protons therefore yields analytical information, since the element type can be determined by the X-ray energy, and its concentration is determined by the X-ray count-rate. PIXE is capable of measuring with high quantitative accuracy elements from sodium and above in the periodic table; detection of X-rays below are not practical because of absorption in the X-ray detector window.

PIXE is similar to the technique of EDX (Energy Dispersive X-ray analysis) used by electron microscopists, where a finely focused beam of electrons is used as the probe. However, the analytical information obtained from an electron beam is degraded by the presence of a high background radiation (called 'bremsstrahlung'); this background is almost absent when using the much heavier proton beam. Fig 3 shows a comparison between a proton induced X-ray energy spectrum and an electron induced X-ray spectrum of a pollen tube tip. As a result of the reduction in background, the nuclear microscope has an analytical sensitivity of parts per million, which is 2-3 orders of magnitude higher than the sensitivity of an analytical electron microscope.

### b) Rutherford Backscattering Spectrometry (RBS)[2]

Although most of the collisions between the incoming proton and the atoms in the sample are with electrons, there is a reduced probability that the incoming proton will collide with an atomic nucleus in the sample. In this case, the incident proton elastically scatters and can rebound back out of the sample. In biological tissue, measurement of the energy of the backscattered proton allows the density and concentration of the matrix elements (eg C, N and O) to be estimated.

c) Scanning Transmission Ion Microscopy (STIM)[3]

For relatively thin samples (eg 30 μm or less), all incident protons that have not suffered backscattering nuclear collisions will pass through the sample. Measurement of the energy of the transmitted protons allows the structure of the sample to be determined through energy loss with atomic electrons. Further, if the protons are measured off-axis (ie off-axis STIM), then the concentrations of hydrogen can be measured.

The NUS nuclear microscope facility[4] is based around a small Van de Graaff ion accelerator (HVEC AN2500) and an Oxford Microbeams OM2000 nuclear microscope endstation, and has a 'state-of-the-art' capability for simultaneous PIXE, RBS and STIM measurements, at a spatial resolution of 0.5 μm. This performance is sufficient to resolve cellular structures in tissue, but in general is not good enough to investigate smaller subcellular features such as organelles. Although further development is in progress to improve the resolution of the nuclear microscope to the 100 nm level, most investigations at the moment are limited to whole cell and tissue analysis. The
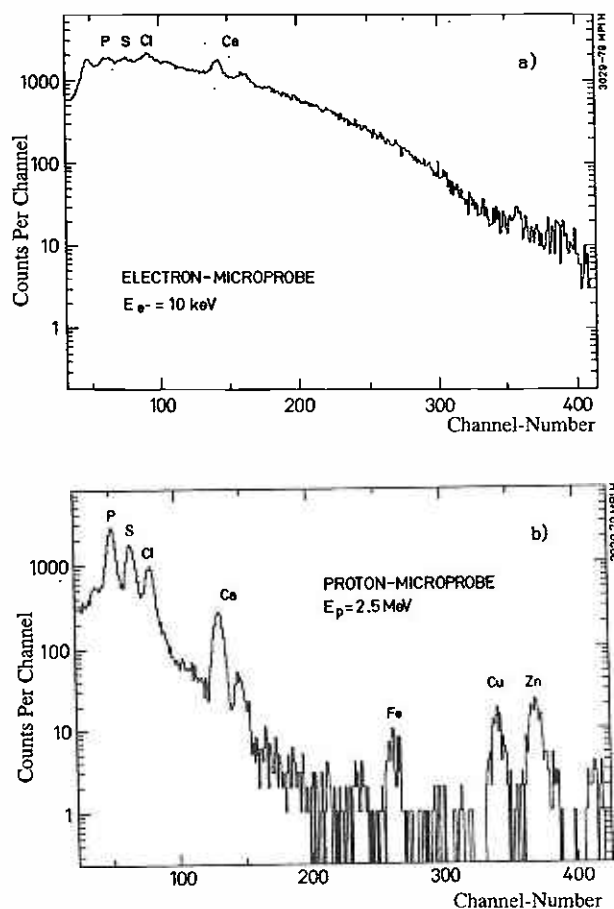
simultaneous utilisation of PIXE, RBS and STIM enables the total elemental analysis of biological tissue to be carried out, from H, C, N and O in the matrix, through the minor elements Na, Mg, P, S, Cl and K, to the trace elements Ca, Fe, Zn and Cu. It must be emphasised that nuclear microscope analyses, unlike many other analytical techniques, can be performed with a high degree of quantitative accuracy. This allows meaningful comparisons of elemental concentrations between different cells and tissue regions. In addition, using sophisticated computer based data acquisition techniques, elemental and structural maps can be generated from information extracted from the PIXE, RBS and STIM data.

The NUS Nuclear Microscopy Group is engaged in a wide variety of interdisciplinary research, ranging from biomedical investigations to micro-electronic device characterisation. In this paper we review briefly the role played by the NUS nuclear microscope in providing analytical information from some of the most common degenerative diseases: atherosclerosis, Parkinson's disease and Alzheimer's disease.

TRANSITION METAL IONS, FREE RADICALS AND DEGENERATIVE DISEASES

Free radicals and oxidative stress have been implicated in many diseases, for example Parkinson's disease[5] and atherosclerosis[6]. While free radicals are essential to normal biochemical processes in the body, free radical mediated damage may also occur through

disruption of membranes, lipids, etc or alteration of enzyme systems and anti-oxidant states, etc[7]. Although free radicals may not be the initial cause of these diseases, they may play an important role in continuing and even accelerating tissue damage[6]. In atherosclerosis, oxidation of low-density lipoproteins are thought to play an important role in atherogenesis. Similar theories apply in Alzheimer's disease[8] and Parkinson's disease in which oxidative damage to dopamine-producing neurons is thought to lead to neuronal cell death[5].

Transition metals ions have been implicated in many diseases through their ability to promote oxidation and reduction chain reactions in which free radicals are produced, leading to a state of oxidative stress. Iron, in particular, can also participate in the Fenton reaction to produce hydroxyl radicals, a highly reactive oxygen species:

$$Fe^{3+} + H_2O_2 \rightarrow Fe^{2+} + OH^- + OH\cdot$$
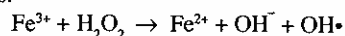
In light of the potential toxicity of transition metal ions in promoting free radical production, it is therefore of interest to study the distribution and concentration of such metal ions in relation to lesioned tissue. Three examples are given here of nuclear microscopic analyses of lesioned tissue in atherosclerosis, Parkinson's disease and Alzheimer's disease.

Atherosclerosis

In atherosclerosis, there is a deposition of hard yellow plaques of lipoid material in the intimal layer of the arteries, coupled with degenerative arterial changes associated with age. This accumulation of atherosclerotic plaques leads to coronary heart disease, one of the leading causes of death. Although various risks factors such as hypercholesterolaemia have been established, the cause of atherosclerosis has yet to be found. Under keen investigation is the Oxidative Modification Theory, as it has been proposed that the oxidative modification of low density lipoproteins (cholesterol carriers in the blood) plays an important role in initiation of atherogenesis[9]. It has been further proposed that free metal ions such as Fe^{2+} and Cu^{2+} catalyse the production of free radicals, leading to the peroxidation of lipids. In addition, iron can also participate in the Fenton reaction to produce hydroxyl radicals, a reactive species involved in the peroxidation of lipids. The Oxidative Modification Theory has been supported by a recent study in the UK[10], where α-tocopherol (vitamin E) treatment was found to substantially reduce the rate of non-fatal myocardial infarction in patients with angiographically proven coronary atherosclerosis. Several epidemiological studies have also been designed to test if there is a relation between body iron and the incidence of heart diseases[11,12] although results of such studies have been mixed and controversial.

Our study focused on investigating the elemental concentrations, particularly that of iron and copper, in atherosclerotic lesions. In this pilot study carried out jointly by the National University of Singapore and the Australian National University, Canberra,[13] atherosclerosis was induced in New Zealand white rabbits. Unstained freeze dried 20 µm sections of the thoracic aorta from 6 test and 4 control rabbits were scanned using the NUS nuclear microscope facility[4]. Fig 4 shows the iron distribution map from a scan on a lesioned artery section. An increase in iron can be seen in the lesion (right side). Table I shows the average elemental concentrations of selected elements extracted from typically 0.5 mm x 0.5 mm scans on the tissue sections. A Student's paired t-test showed a significant increase in P and Fe and a significant decrease in S, Cl, K, Ca and Zn at the 95% confidence level. There is a seven-fold increase in iron in the lesion and this adds weight to the hypothesis that iron-catalysed free radical reactions could play a role in initialising

Fig 4 – Iron distribution map from a 600 µm x 600 µm scan of a lesioned artery section. The right edge of the scan corresponds to the inner wall of the artery. An increase in Fe is seen in the lesioned tissue (right half) compared to the healthy tissue (left half).
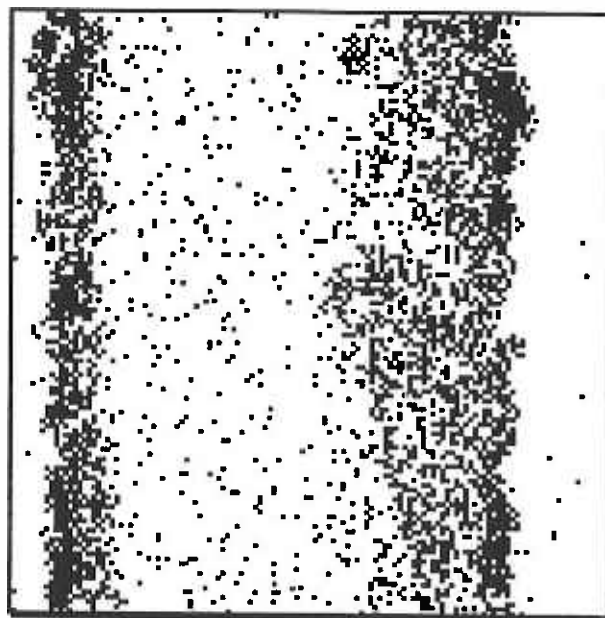

Table I – Average elemental concentrations in lesioned and control rabbit artery tissue sections

	(1) Lesion	(2) Healthy	(3) Ratio	(4) Controls
P	6190 (686)	3558 (397)	1.8 (0.1)	3227 (378)
S	4681 (304)	7589 (716)	0.64 (0.06)	6803 (393)
K	2004 (342)	2494 (417)	0.81 (0.04)	2968 (504)
Ca	543 (39)	842 (54)	0.65 (0.05)	639 (95)
Fe	84 (20)	12.5 (2.2)	7.4 (1.4)	23 (13)
Cu	4.7 (0.2)	5.0 (1.1)	0.8 (0.3)	3.5 (0.7)
Zn	50 (9)	101 (13)	0.51 (0.09)	141 (36)

Average concentrations (parts per million, dry weight) of selected elements in lesioned tissue (column 1), healthy tissue adjacent to the lesion (column 2) from 6 cholesterol fed rabbits, and in healthy tissue from 4 control rabbits (column 4). The average elemental ratios between lesioned and healthy tissue from test rabbits are shown in column 3. Standard errors are shown in parentheses.

the onset of atherosclerosis. Work is in progress to investigate the elemental changes as a function of time from the onset of lesioning so as to deduce whether the observed changes in elemental concentrations are causative in nature or are effects of atherosclerotic lesioning. Histochemical analysis of serial sections will also be carried to complement the information obtained from the nuclear microscopic analysis so as to shed some light on the role of iron in atherogenesis.

Parkinson's Disease

Parkinson's disease is characterised by a loss of dopamine-producing cells in the substantia nigra (SN), particularly in the pars compacta region (SNc), resulting in impairment of the motor system. Other characteristics such as changes in mitochondrial function, iron metabolism and glutathione levels have also been established[14]. However, the cause of dopaminergic cell death in the SN remains unknown. Based on the ability of iron ions to participate in oxidation and reduction reactions in which free radicals are generated, researchers have proposed a role for iron-

mediated free radical reactions leading to a state of oxidative stress in the brain [see introduction in[5]]. Indeed, dopaminergic neurons may be particularly susceptible to free radical damage for the reasons that the substantia nigra region is known to be rich in iron, free radicals are generated in the metabolism of dopamine and that neuromelanin granules in the Parkinsonian SN have been shown to accumulate iron compared to controls[15].

In our study conducted jointly by the National University Hospital and NUS Nuclear Microscopy Group, we investigated the distributions and concentrations of iron in the SN of rat parkinsonian brain tissue. Male Sprague-Dawley rats unilaterally injected with 6-hydroxydopamine (6-OHDA) were used as an animal model[16]. The lesioned rats were tested for rotational response to amphetamine and only rats exhibiting turning rates of 7 turns/min or more were selected as successful animal models[17]. Both test and control rats (injected with ascorbic acid) were sacrificed after one year and unstained freeze dried 20 µm sections of the brain encompassing the entire SN were analysed using the NUS Nuclear Microscope facility[4]. Fig 5 shows the iron map from a scan of a 6-OHDA lesioned brain section encompassing the entire SN. Three pin-holes used to mark the extremities of the SN prior to sectioning can be seen. These holes, together with the inherent higher iron content in the SN facilitated the identification of the entire SN during data analysis. Table II shows the average iron concentrations in the SN and surrounding tissue in 7 test and 8 control rates. A Student's t-test performed at the 95% confidence level showed a significant increase in iron concentrations (26%) in the right (lesioned) SN compared to the left (non-lesioned) SN in test rats. An increase of 31% was also seen in the tissue surrounding the SN. Such an elevation of iron was not seen in the control rats either in the SN or surrounding tissue.

Our results agree with the results of Oestricher et al[18] who reported a 35% increase in iron concentrations in the SN of rats unilaterally lesioned with 6-OHDA. The increase in iron in lesioned SNs imply that it may be involved in the degeneration process in Parkinson's disease. However, since accumulation of iron is not specific to Parkinson's disease (it has been observed in other diseases affecting the basal ganglia), and our results show that there is also an increase in iron in the tissue surrounding the SN, iron accumulation may not be a cause of dopaminergic cell death but rather a product of a pathological process. Current work focuses on using MPTP-lesioned monkeys as a primate model for parkinsonism. Preliminary results also showed an increase in iron in the MPTP-lesioned SN. By monitoring changes in elemental concentrations in the SN as a function of time starting from lesioning, we hope to shed light on the role of iron in dopaminergic cell death.

Aluminium in Neurofibrillary Tangles in Alzheimer's Disease

Alzheimer's disease (AD) is the most common form of senile dementia, affecting up to 25% of the population above 80 years of age. It is a progressive neurodegenerative disease of unknown origin. Aluminium has been proposed as a possible cause of AD, but the data presented is far from being conclusive[19]. It is also suggested that iron and free radicals may play a key role[8,20].

Pathologically, AD is characterized by two main types of lesions, neuritic plaques and neurofibrillary tangles (NFTs), which occur in several areas of the brain. Increased Al levels have been found both in neuritic plaques[21] and NFTs[22], which is so far the most direct link between Al and AD. However, these results are neither consistent nor readily reproducible; furthermore, they were obtained by analysing fixed and stained tissue. The work of Landsberg et al [23] has shown that chemical treatment of tissue prior to the analysis leads to tissue contamination with aluminosilicates. They used nuclear

Fig 5 - Map from a 2.4 mm x 2.4 mm scan of a brain section from a 6-OHDA lesioned rat showing the distribution of iron. The substantia nigra (SN) can be identified both by the three marker pin-holes and its inherently high iron content.
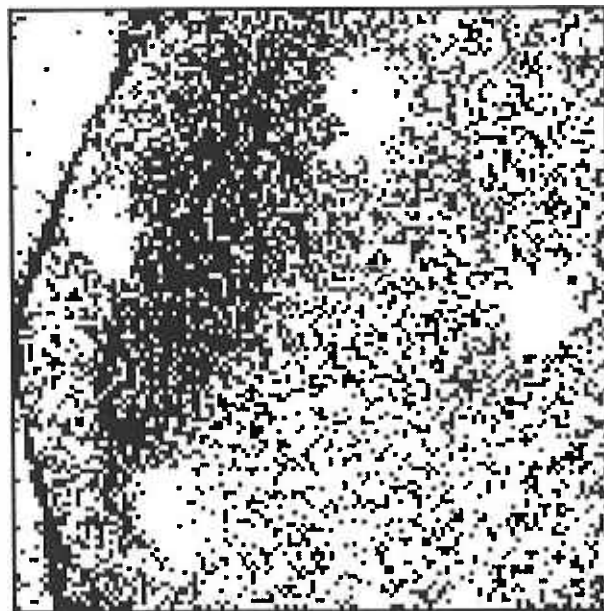

Table II – Average iron concentrations in lesioned and control rat brain tissue sections.

| | 6-OHDA Lesioned Rats (n=7) | | Control Rats (n=8) | |
	SN	Surrounding	SN	Surrounding
Right brain	294 (27.6)	91.2 (13.7)	242 (26.9)	78.3 (5.8)
Left brain	234 (21.2)	68.8 (7.1)	235 (24.9)	76.7 (6.2)
Ratio	1.26 (0.06)	1.31 (0.08)	1.03 (0.04)	1.03 (0.05)

Average iron concentrations (parts per million, dry weight) in the substantia nigra (SN) and surrounding tissue obtained from 7 6-OHDA lesioned and 8 control rats. The average ratios of the concentrations between that found in the right (injected) and left brains in individual rats are also shown. All standard errors are shown in parentheses.

microscopy to determine Al levels in neuritic plaques in flash frozen tissue which has not been chemically treated in any way, as well as in flash frozen tissue which has been immuno-histochemically stained. Due to the difference in density between the amyloid-rich plaques and the surrounding tissue, plaques were identified by STIM in thin sections. Simultaneous application of STIM, PIXE and RBS enabled total elemental analysis of the tissue. Aluminium was not detected in any of more than 100 plaques in unstained flash frozen tissue at the detection limit of 15 ppm. On the other hand, immunohistochemically stained AD sections showed Al presence above the detection limit in 10% of the analysed plaques, implying that Al has been introduced as a contaminant during the staining procedures.

The current project at the NUS involves a similar experiment with NFTs. NFTs are bundles of paired helical filaments composed of abnormally phosphorylated tau protein which develop within the affected neurons. Neurons are up to 10 times smaller than neuritic plaques which make their STIM imaging much more difficult. Nevertheless, the experiments performed on the AD tissue so far show that it can be done. Neurons have higher density compared to supporting tissue and NFTs have, in turn, higher density than the neurons. Consequently, it is possible to localise neurons by STIM imaging and also to identify the

NFT-bearing neurons. So far, this procedure has only been carried out on samples which have undergone extensive treatment. Brains of AD patients were obtained post mortem and fixed in 10% formalin. Small blocks were cut from the hippocampus A1 region, osmicated and embedded in spurr resin. From these blocks 2 µm thick sections were cut, placed on pioloform-coated slides and stained with toluidine blue for several minutes on a hot plate before being rinsed with distilled water to terminate the staining process. The pioloform films with stained sections were subsequently floated off in distilled water and picked up on target holders suitable for analysis with nuclear microscope.

The sections were scanned with a 10 pA 2 MeV proton beam at spatial resolutions close to 100 nm. After scanning 200 µm x 200 µm areas to localise neurons, the scan size was reduced to 20-50 µm, depending on neuron size and position. Data were collected for approximately 1 hour and stored in the computer so that the STIM energy loss window could be optimised for maximum contrast during off-line analysis. Fig 6 shows one of the NFT-bearing neurons, part of which was imaged in a 30 µm x 30 µm scan. The outline of the neuron is shown against the background tissue which is denser on one side (DT). The nucleus (N) and the neurofibrillary tangle (NFT) are also seen as darker regions within the neuron.

This work will be continued on flash-frozen tissue which has not been fixed or stained. The unique feature of STIM to image neurons in untreated tissue will be used to simultaneously localise normal and NFT- bearing neurons and determine their elemental compositions using PIXE and RBS. These results therefore will not be subject to misinterpretation due to contamination.

Fig 6 – A 30 µm x 30 µm STIM image of a neuron, showing a neurofibrillary tangle (NFT) and the nucleus (N). DT indicates the dense surrounding tissue.
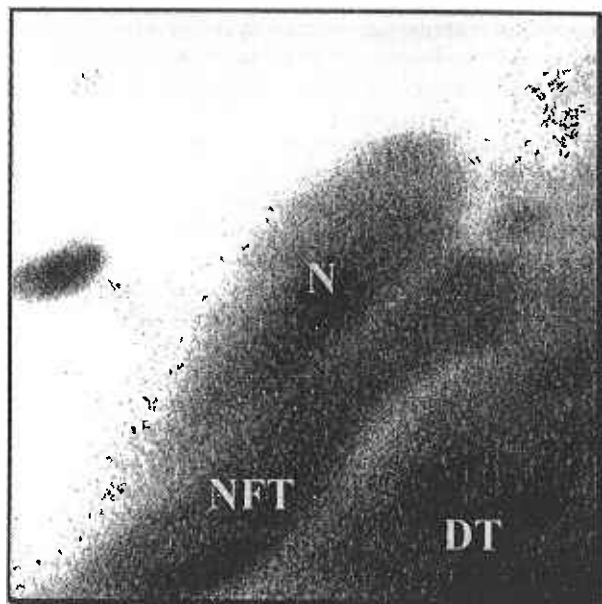
REFERENCES

1. Johansson SAE, Campbell JL, Malmqvist KG, editors. Particle induced X-ray emission spectrometry. Chemical analysis series Vol. 133. New York: John Wiley, 1995.

2. Chu WK, Mayer JW, Nicolet MA. Backscattering spectrometry. New York: Academic, 1978.

3. Overley JC, Connolly RC, Seiger GE, McDonald JD, Lefevre HW. Energy-loss radiography with a scanning MeV-ion microprobe. Nucl Instr and Meths 1983; 218: 43-6.

4. Watt F, Orlic I, Loh KK, Sow CH, Thong P, Liew SC, et al. The National University of Singapore nuclear microscope facility. Nucl Instr & Meth 1994; B85: 708-15.

5. Olanow CW. An introduction to the free radical hypothesis in Parkinson' disease. Ann Neurol 1992; 32 (Suppl): S2-S9.

6. Halliwell B. The role of oxygen radicals in human disease, with particular reference to the vascular system. Haemostasis 1993; 23 Suppl 1: 118-26.

7. Rice-Evans C, Burdon R. Free radical-lipid interactions and their pathological consequences. Prog Lipid Res 1993; 32(1): 71-110.

8. Borman S. Alzheimer's disease: Free-radical reactions may play key role. C&EN 1994; April 18: 4-5.

9. Steinberg D, Parthasarathy S, Carew TE, Khoo JC, Witztum JL. Beyond cholesterol: Modifications of low-density lipoproteins that increase its atherogenicity. N Engl J Med 1989; 320: 915-24.

10. Stephens NG, Parsons A, Schofield PM, Kelley F, Cheeseman K, Mitchinson J, et al. Randomised controlled trial of vitamin E in patients with coronary disease: Cambridge Heart Antioxidant Study (CHAOS). Lancet 1996; 347: 781-6.

11. Salonen JT, Nyyssonen K, Korpela H, Tuomilehto J, Seppanen R, Salonen R. High stored iron levels are associated with excess risk of myocardial infarction in Eastern Finnish men. Circulation 1992; 86(3): 803-11.

12. Liao Y, Cooper RS, McGee DL. Iron status and coronary heart disease: negative findings from the NHANES I epidemiologic follow-up study. Am J Epidemiol 1994; 139(7): 704-12.

13. Thong PSP, Selley M, Watt F. Elemental changes in atherosclerotic lesions using nuclear microscopy. Cell Mol Biol 1996; 42(1): 103-10.

14. Jenner P. Altered mitochondrial function, iron metabolism and glutathione levels in Parkinson's disease. Acta Neurol Scand 1993; 87 Suppl. 146: 6-13.

15. Good PF, Olanow CW, Perl DP. Neuromelanin-containing neurons of the substantia nigra accumulate iron and aluminium in Parkinson's disease: a LAMMA study. Brain Res 1992; 593: 343-6.

16. He Y, Thong PSP, Lee T, Leong SK, Shi CY, Wong PTH, et al. Increased iron in the substantia nigra of 6-OHDA induced Parkinsonian rats: A nuclear microscopy study. Brain Res 1996. (In press)

17. Dexter DT, Wells FR, Lee AJ, Agid Y, Jenner P, Marsden CD. Increased nigral iron content and alterations in other metal ions occurring in brain in Parkinson's disease. J Neurochem 1989; 52: 1830-6.

18. Oestricher E, Sengstock GJ, Riederer P, Olanow CW, Dunn AJ, Arendash GW. Degeneration of nigrostriatal dopaminergic neurons increases iron within the substantia nigra: a histochemical and neurochemical study. Brain Res 1994; 660: 8-18.

19. Doll R. Review: Alzheimer's disease and environmental aluminium. Age Aging 1993; 22: 138-53.

20. McDonald B, Landsberg JP, Grime GW, Watt F. Elemental analysis of neuritic plaque cores in Alzheimer's disease using nuclear microscopy. Life Chemistry Report 1994; 11: 41-5.

21. Candy JM, Klinowski J, Perry RH, Perry EK, Fairbairn A, Oakley AE, et al. Aluminosilicates and senile plaque formation in Alzheimer's disease. Lancet 1986; 354-7.

22. Good PF, Perl DP, Bierer LM, Schmeidler J. Selective accumulation of aluminium and iron in the neurofibrillary tangles of Alzheimer's disease: A laser microprobe (LAMMA) study. Ann Neurol 1992; 31 (3): 286-92.

23. Landsberg JP, McDonald B, Watt F. Absence of aluminium in neuritic plaque cores in Alzheimer's disease. Nature 1992; 360: 65-7.